

Revisiting receiver temperature (T_{rxr}) measurements using auto-correlations.

Bharat Kumar Gehlot, Danny Jacobs, Tyler Cox, Shane Bechtel

May 15, 2019

1 Introduction

In this memo, we revisit the method to calculate receiver temperature T_{rxr} of HERA proposed by Adam Beardsley in HERA Memo#16. In this method, auto-correlations from different antennas are fitted to a pre-calculated Sky temperature template produced by integrating a known sky model (Global Sky Model in our case) multiplied with known HERA beam model. The fitted gain and noise bias terms are used to determine T_{rxr} .

2 Methodology

Auto-correlations (same polarization) $R(\nu, t)$ measured by an antenna can be written as

$$R(\nu, t) = g(\nu) \times T_{\text{sky}}(\nu, t) + N \quad (1)$$

where $g(\nu)$ is frequency dependent receiver gain (assumed to be stable in time), $T_{\text{sky}}(\nu, t)$ is the sky temperature integrated over the beam and N is the noise bias due to the receiver temperature $T_{\text{rxr}}(\nu)$ which can be estimated from $g(\nu)$ and N as:

$$T_{\text{rxr}}(\nu) = \frac{N}{g(\nu)} \quad (2)$$

We fit the auto-correlation data to the known sky temperature model to obtain $g(\nu)$ and N .

2.1 Data and model selection

We use H1C (HERA-47, with old PAPER feeds) and H2C (new Vivaldi feeds) datasets with IDs H1C-IDR2.1 2458116, H2C 2458536, 2458551, 2458560 for sky temperature fitting. We use GSM 2008 model to generate the sky temperature model using the Dipole and Vivaldi beam models¹ by Nicholas Fagnoni. By default (as in Memo#16), the sky temperature template is calculated at 30 mins and 1 MHz resolution.

2.2 Template fitting

We use the following template to fit the auto-correlation data for G_0 and N_0 :

$$\text{template[LST]} = G_0 \times (T_{\text{sky}} - \langle T_{\text{sky}} \rangle_{\text{LST}}) + N_0 \quad (3)$$

The fit parameters \hat{G}_0 and \hat{N}_0 are obtained per frequency channel and can be converted to \hat{T}_{rxr} as

$$\hat{T}_{\text{rxr}} = \frac{\hat{N}_0}{\hat{G}_0} - \langle T_{\text{sky}} \rangle \quad (4)$$

Variance (σ_T^2) of the \hat{T}_{rxr} estimate can be calculated using the Covariance matrix of \hat{G}_0 and \hat{N}_0 using the following relation:

$$\left(\frac{\sigma_T}{\hat{T}_{\text{rxr}}} \right)^2 = \left(\frac{\sigma_{GG}}{\hat{G}_0} \right)^2 + \left(\frac{\sigma_{NN}}{\hat{N}_0} \right)^2 - 2 \left(\frac{\sigma_{NG}}{\hat{N}_0 \hat{G}_0} \right)^2 \quad (5)$$

where σ_{GG} and σ_{NN} are the diagonal terms of the covariance matrix and correspond to the error on \hat{G}_0 and \hat{N}_0 , respectively. σ_{NG} is one of the off-diagonal terms of the same covariance matrix. Equation 1 can be rearranged to obtain \hat{T}_{sky} from auto-correlations $R(\nu, t)$ using the fitting parameters as:

$$\hat{T}_{\text{sky}}(\nu, t) = \frac{R(\nu, t)}{\hat{G}_0(\nu)} - \hat{T}_{\text{rxr}}(\nu) \quad (6)$$

¹Github repo:<https://github.com/HERA-Team/HERA-Beams>

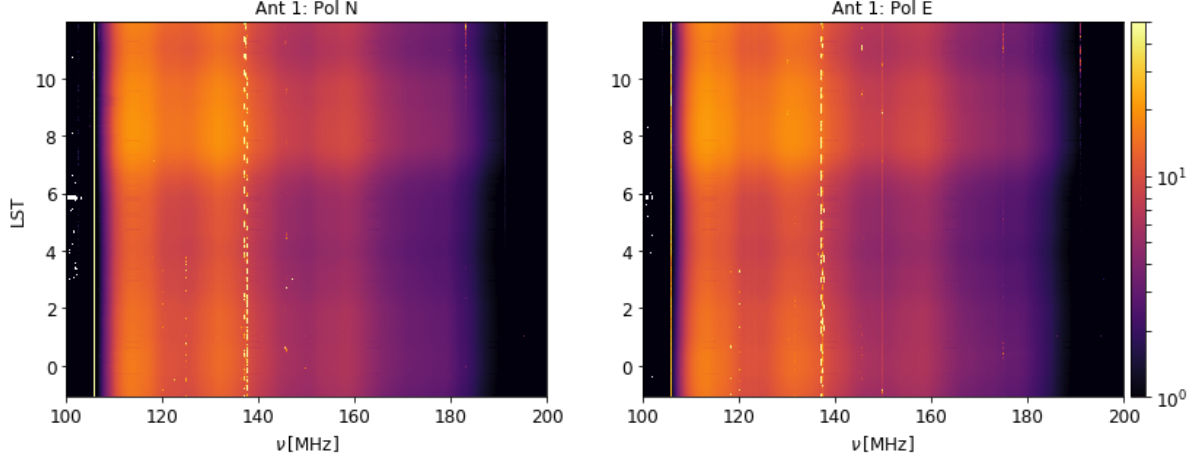


Figure 1: Antenna 1 auto-correlations for two polarizations ‘N’ (left column) and ‘E’ (right column) from observation H1C-IDR2.1-2458116.

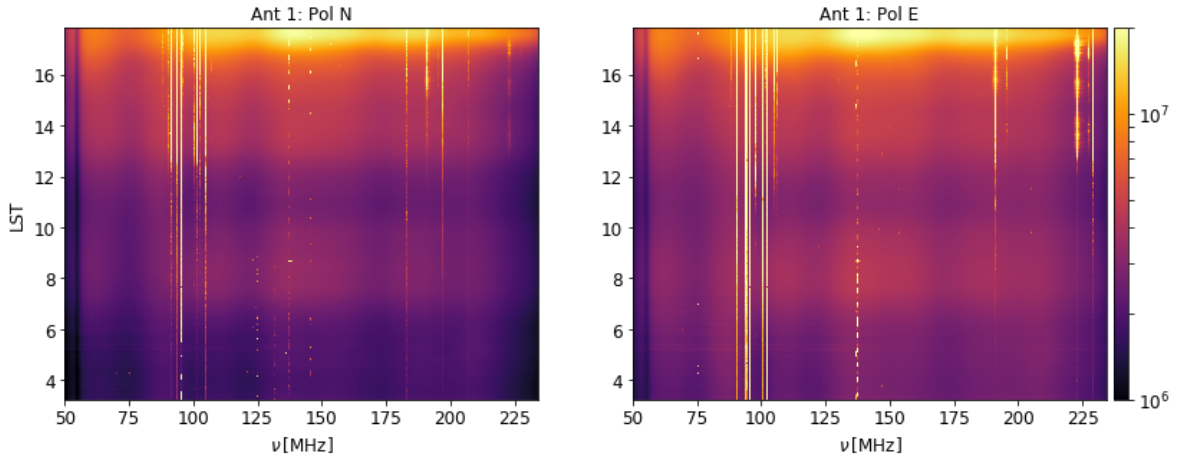


Figure 2: Same as figure 1 but for H2C-2458560 observation.

The script to perform the fitting task is maintained as a jupyter notebook on github repository https://github.com/tacox5/HERA_Tsys. Fitting is performed per frequency channel and does not account for RFI i.e. no RFI-flagging is performed before or during fitting.

3 Fitting results

Figure 1 shows antenna 1 auto-correlations for two polarizations ‘N’ (left column) and ‘E’ (right column) from observation H1C-IDR2.1-2458116. Similarly, Figure 2 shows antenna 1 auto-correlations from observation H2C-2458560.

3.1 H1C data results

We use HERA-47 (H1C-IDR2.1-2458116) data to estimate \hat{T}_{rxr} . The T_{sky} template used for this fit has a time and frequency resolution of 30 minutes and 1 MHz, respectively. Figures 3 and 4 show \hat{T}_{sky} obtained from antenna 1 auto-correlations, the T_{sky} template used for fitting (model) and the residuals $((\hat{T}_{\text{sky}} - T_{\text{sky}})/T_{\text{sky}})$. We observe that residuals are closer to zero in 2-10 hours LST range but deviate from zero otherwise. RFI affected LSTs are clearly visible in residuals. It should be noted that residuals are more or less constant in frequency direction.

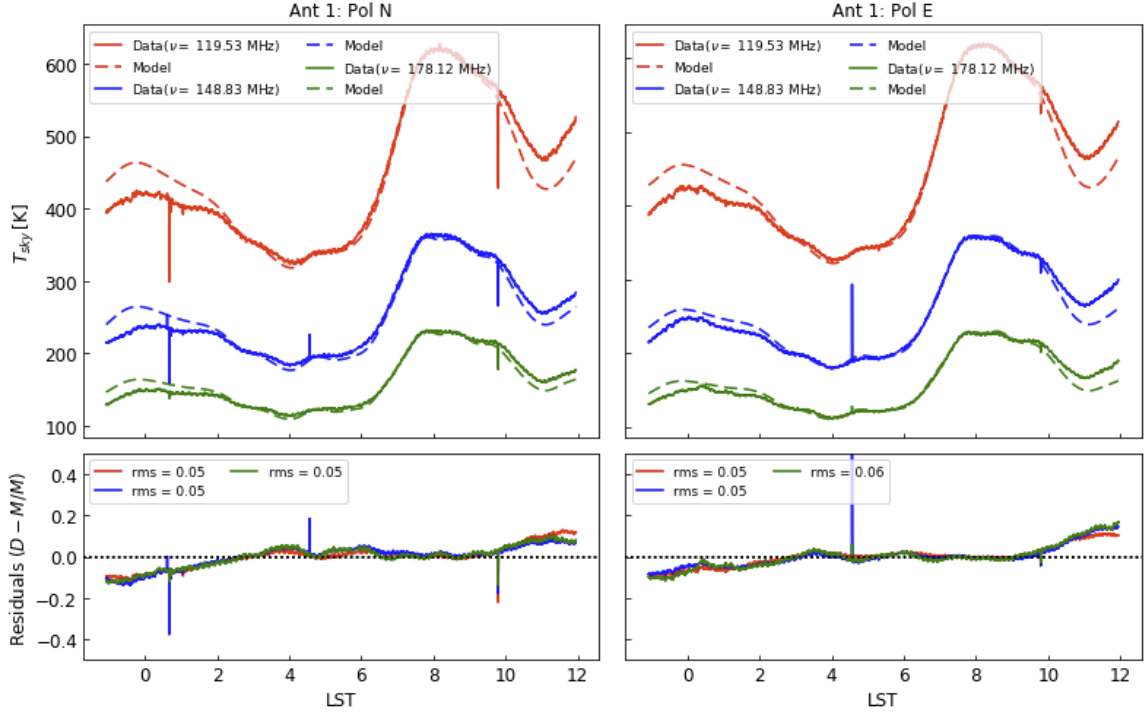


Figure 3: Top panel: \hat{T}_{sky} (data) estimated from antenna 1 auto-correlations of H1C-2458116 data and T_{sky} template as a function of LST for three different frequency channels. Bottom panel: Fractional residuals $(\hat{T}_{\text{sky}} - T_{\text{sky}})/T_{\text{sky}}$ corresponding to the three channels shown in top panel.

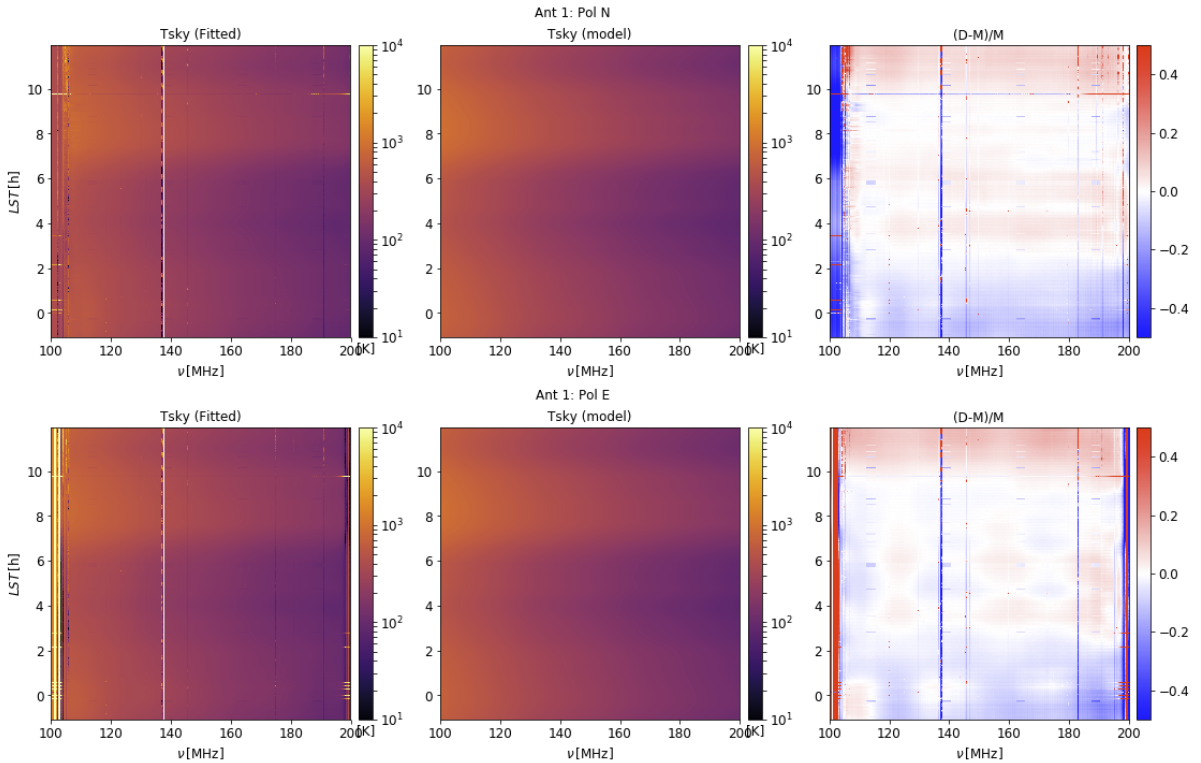


Figure 4: Left column: Waterfall plot of \hat{T}_{sky} estimated from antenna 1 auto-correlations of H1C-2458116 data. Middle Column: waterfall plot of T_{sky} template. Right column: fractional residuals corresponding to left and middle columns.

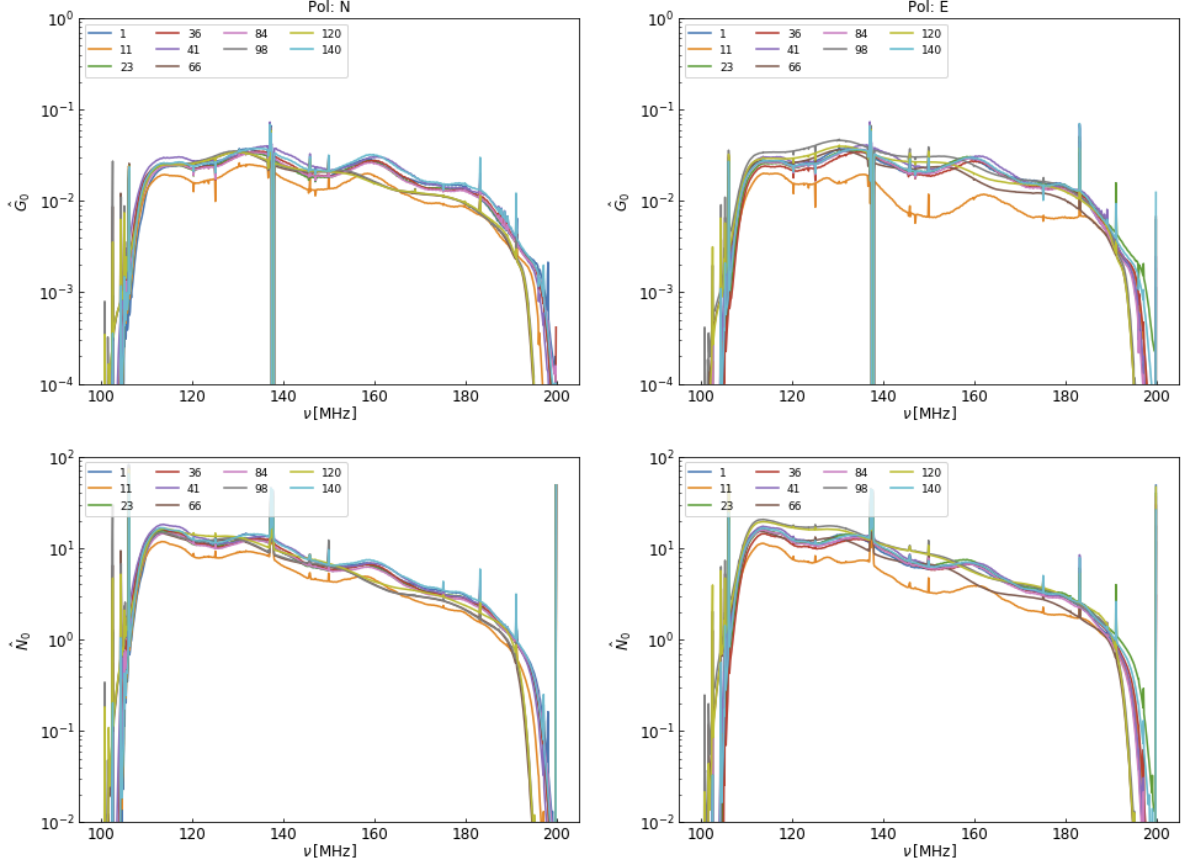


Figure 5: Left column: fitted parameters \hat{G}_0 (top panel) and \hat{N}_0 (bottom panel) for different antennas for ‘N’ polarization (H1C-2458116 data). Right column: Same as left column but for ‘E’ polarization.

The fitting parameters \hat{G}_0 and \hat{N}_0 for different antennas and polarizations are shown in figure 5 for several antennas and the two polarizations. We observe that \hat{G}_0 and \hat{N}_0 each are similar for different antennas, except for a few outliers. However, both \hat{G}_0 and \hat{N}_0 exhibit a ripple in frequency direction, although only \hat{G}_0 is expected to exhibit such ripple. This might be primarily due to covariance between the two parameters.

Figure 6 shows \hat{T}_{RXR} (top row) obtained from auto-correlation fitting and the errors on \hat{T}_{RXR} estimates (bottom row). We notice that \hat{T}_{RXR} are similar for most antennas. However, the estimated values are surprisingly lower than the estimates from lab measurements. The values are lower than 100 K over most of the frequency band and goes as low as 10 K (even negative for some antennas) which is highly unrealistic. The errors on these values are also underestimated and are of order of 5-10%. Using incorrect sky model and/or imperfect beam model to calculate T_{sky} template can affect the fitting process and might lead to wrong results. Deviation of the fit from the data for LSTs before 2 hours or after 10 hours as observed in figures 3 and 4 suggests that sky-model for those LSTs is not accurate enough for the fitting task. As mentioned in section 2.1, the T_{sky} template used for fitting task was calculated at 30 minutes and 1 MHz resolution and is linear interpolated to match time and frequency resolution of HERA. This might introduce errors in the fitting task and produce bias in the final \hat{T}_{RXR} estimate. However, using a higher resolution T_{sky} template (2 minutes and 200 kHz resolution) does not affect H1C results.

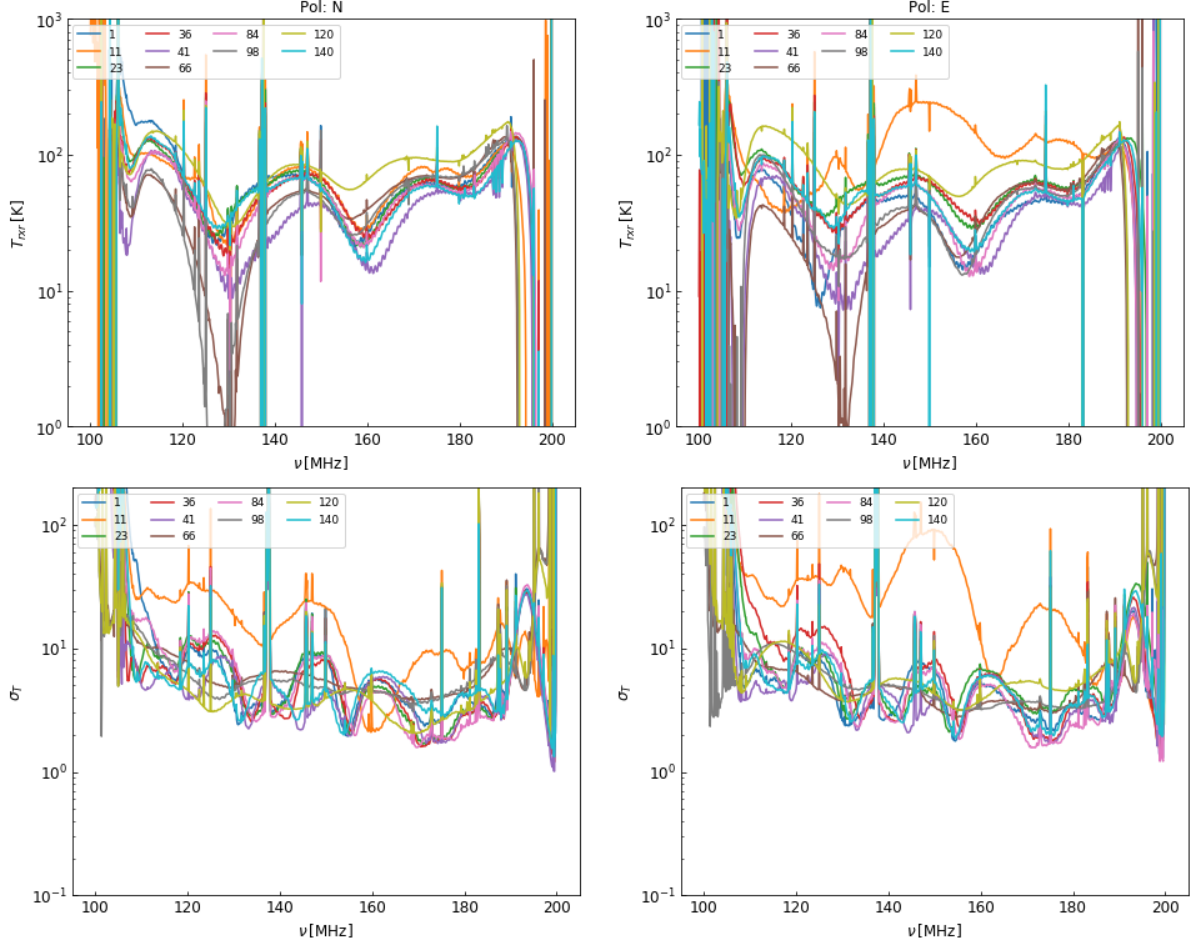


Figure 6: Top row: \hat{T}_{rxr} for different antennas for ‘N’ and ‘E’ polarizations (left and right panels, respectively) estimated from H1C-2458116 data. Bottom row: Error (σ_T) on \hat{T}_{rxr} shown in top row.

3.2 H2C data results

In this section, we estimate \hat{T}_{rxr} for the new Vivaldi feeds from H2C datasets using the fitting method described earlier. We noticed that changing the resolution of the T_{sky} template affects the fitting results significantly for the H2C data. Therefore, we use a template with time and frequency resolution of 2 minutes and 200 kHz for fitting receiver temperatures. Here we show results from H2C-2458560 data.

Figures 7 and 8 show \hat{T}_{sky} obtained from antenna 1 auto-correlations, the T_{sky} template used for fitting (model) and the residuals ($(\hat{T}_{\text{sky}} - T_{\text{sky}})/T_{\text{sky}}$). We observe a trend that the fit is worse for ‘N’ polarization compared to ‘E’ polarization for all antennas (only antenna 1 is shown here). RMS values of fractional residuals for ‘N’ polarization are factor of 2-3 higher than that of ‘E’. A poor beam model for ‘N’ polarization might be a possible reason that can be the cause of the poor fitting compared to ‘E’. Moreover, fractional residuals in H2C data exhibit periodic structure along frequency direction compared to H1C data.

Figure 9 shows fitting parameters for different antennas (both polarizations) estimated from H2C-2458560 auto-correlations. We observe that both \hat{G}_0 and \hat{N}_0 for ‘E’ polarization of different antennas agree with each other. Whereas, ‘N’ polarization have antenna-to-antenna variation in amplitudes of \hat{G}_0 and \hat{N}_0 . The \hat{N}_0 estimates for different antennas are relatively constant along frequency, whereas \hat{G}_0 values are smaller at lower frequencies. Figure 10 shows \hat{T}_{rxr} estimated from H2C-2458560 auto-correlations. We observe that \hat{T}_{rxr} are ~ 200 K at frequencies higher than 130 MHz. This is almost twice higher compared to lab measurements ($\hat{T}_{\text{rxr}} \sim 100$ K). It is

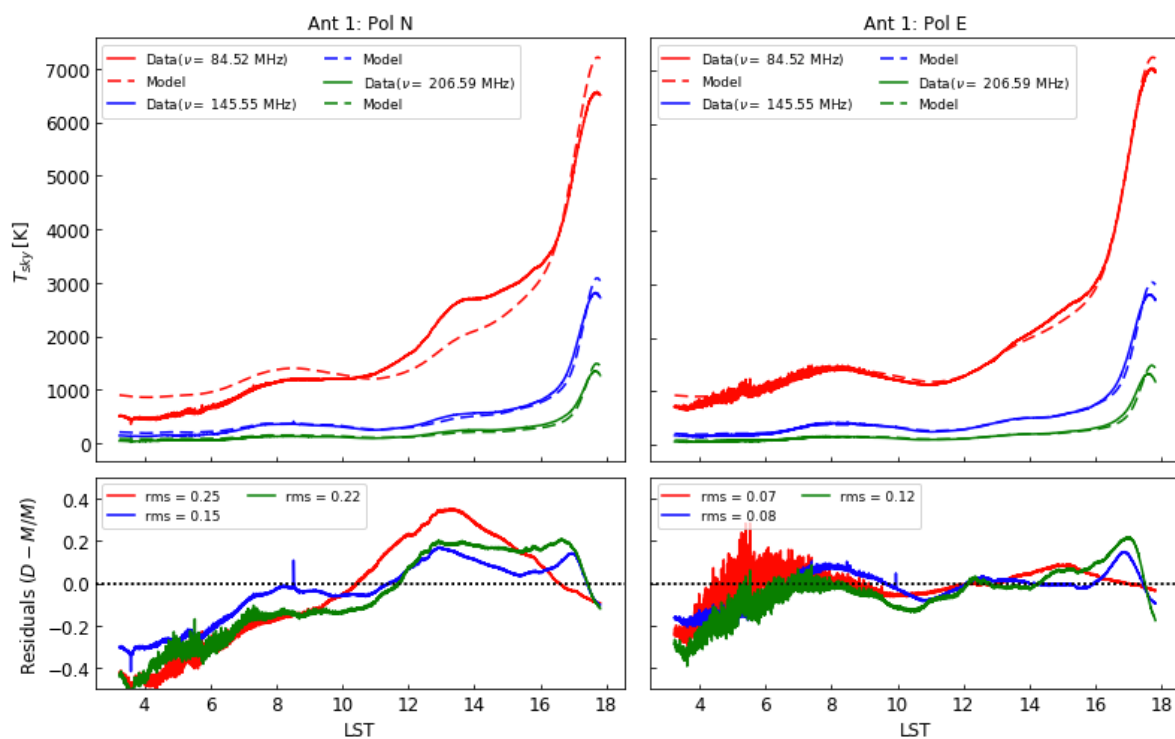


Figure 7: Same as figure 3 but for H2C-2458560 data.

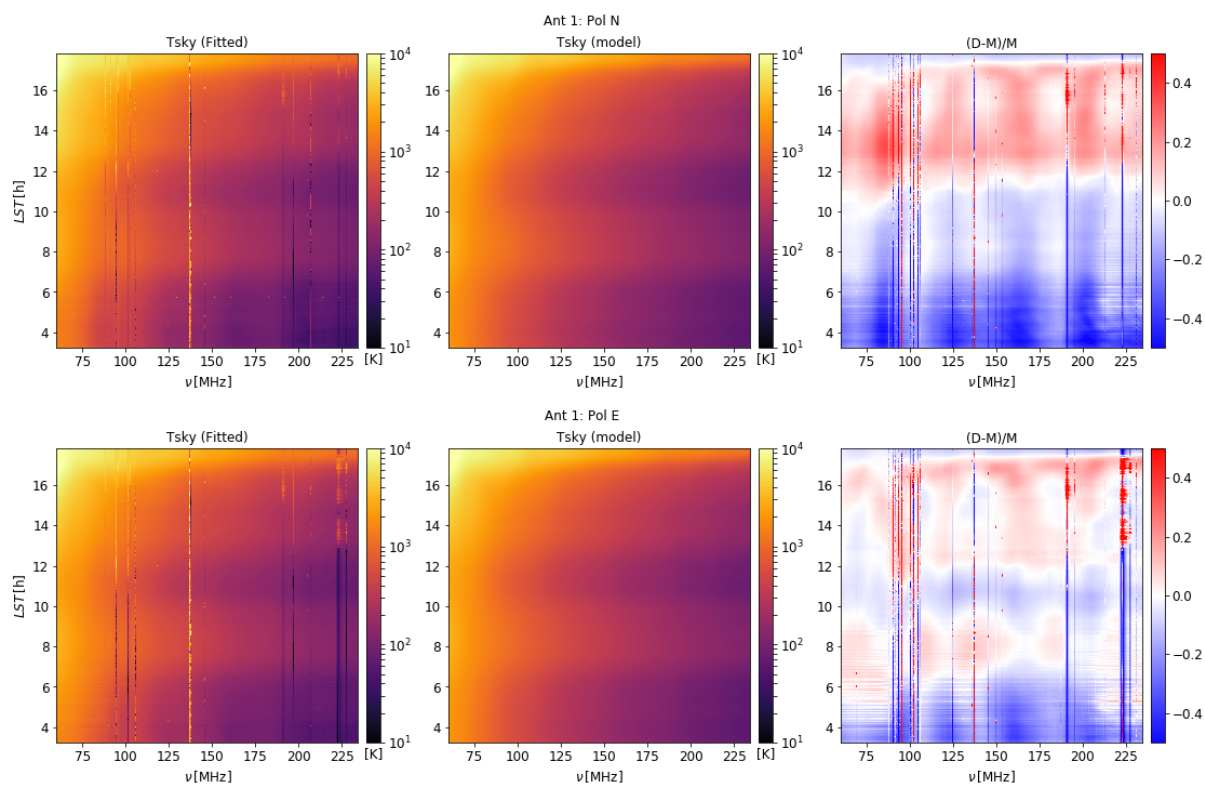


Figure 8: Same as figure 4 but for H2C-2458560 data.

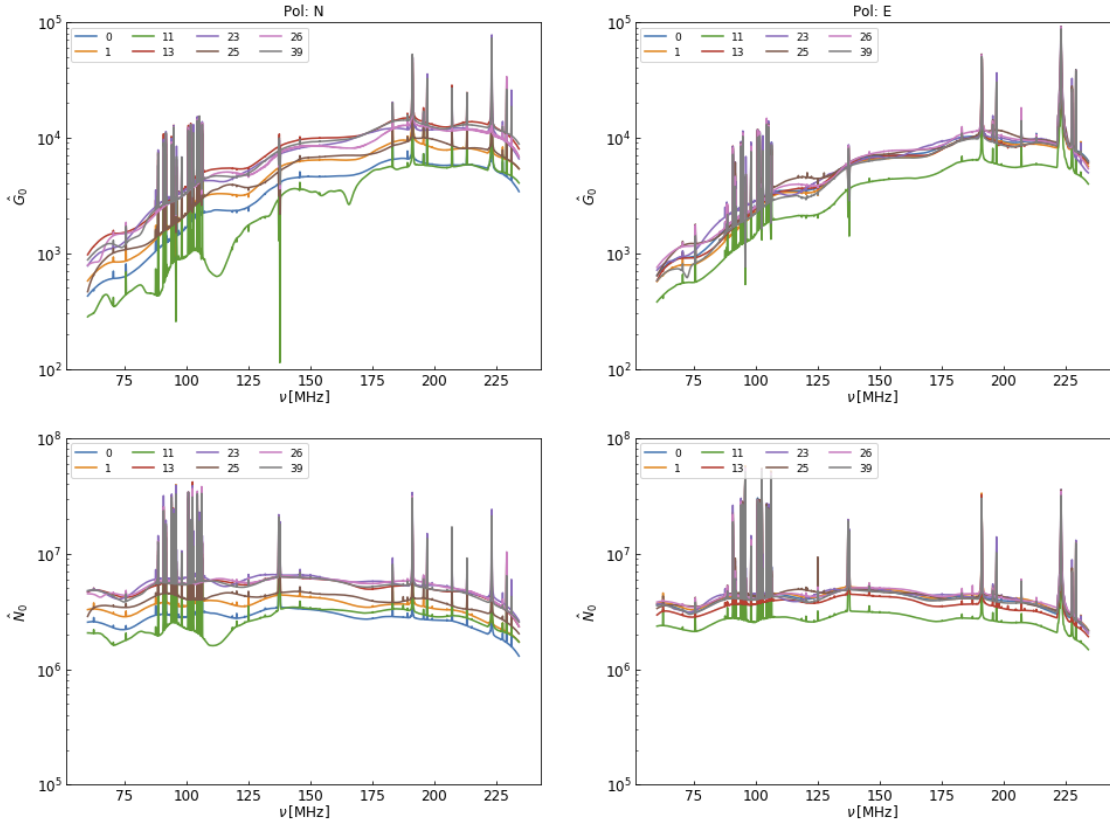


Figure 9: Same as figure 5 but for H2C-2458560 data.

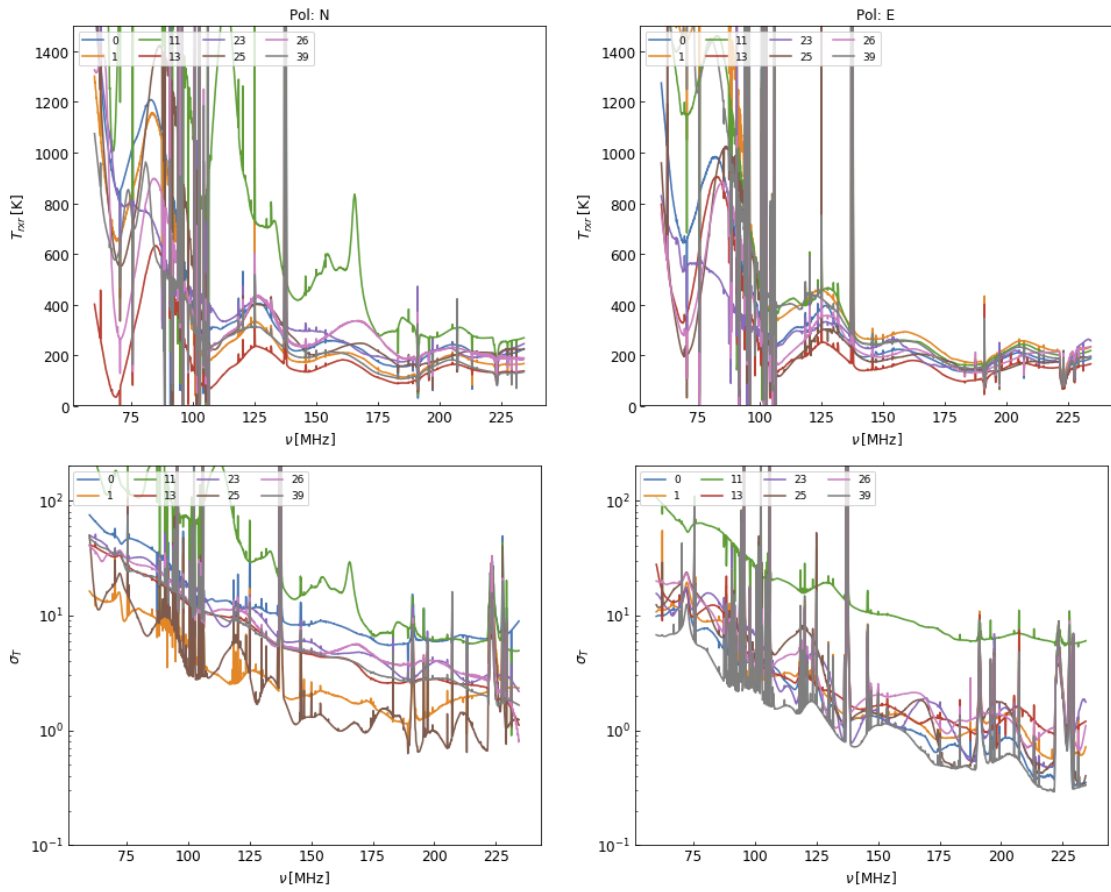


Figure 10: Same as figure 6 but for H2C-2458560 data.

difficult to trust \hat{T}_{rxr} for frequencies less than 130 MHz because the beam model is imperfect at low frequencies. The errors on \hat{T}_{rxr} estimates are of the order of few %.

4 Conclusion

In this memo, we estimate \hat{T}_{rxr} from auto-correlations data of H1C-IDR2.1-2458116 and H2C-2458560 observations. We observe that \hat{T}_{rxr} values for H1C data are lower (and sometimes unrealistic) than expected. Whereas, \hat{T}_{rxr} values for H2C data are around twice (or more) higher than expected over most of the frequency band. Main reasons behind wrong \hat{T}_{rxr} estimates and underestimated error bars might be the incomplete sky-model and/or imperfect beam model used to generate the T_{sky} template. In next memo, we'll use simulations to understand the cause of these issues in more detail.